Available online at www.sciencedirect.com
ScienceDirect
Journal of Power Sources 161 (2006) 813–819
JOURNAL OF POWER SOURCES
www.elsevier.com/locate/jpowsour

$PtRuO_2$/Ti anodes with a varying Pt:Ru ratio for direct methanol fuel cells

Zhi-Gang Shao [a,b,*], Fuyun Zhu [a,1], Wen-Feng Lin [a,**], Paul A. Christensen [a], Huamin Zhang [b]

[a] *School of Chemical Engineering and Advanced Materials, Bedson Building, University of Newcastle upon Tyne, Newcastle upon Tyne NE1 7RU, UK*
[b] *Dalian Institute of Chemical Physics, Chinese Academy of Sciences, China*

Received 13 March 2006; received in revised form 22 May 2006; accepted 6 June 2006
Available online 27 July 2006

Abstract

$PtRuO_2$/Ti anodes with a varying Pt:Ru ratio were prepared by thermal deposition of a $PtRuO_2$ catalyst layer onto a Ti mesh for the direct methanol fuel cell (DMFC). The morphology and structure of the catalyst layers were analyzed by SEM, EDX, and XRD. The catalyst coating layers became porous with increase of the Ru content, and showed oxide and alloy characteristics. The relative activities of the $PtRuO_2$/Ti electrodes were assessed and compared using half-cell tests and single DMFC experiments. The results showed that these electrodes were very active for the methanol oxidation and that the optimum Ru surface coverage was ca. 38% for a DMFC operating at 20–60 °C.

Keywords: DMFC; Pt:Ru ratio; $PtRuO_2$/Ti anodes; Ti mesh

1. Introduction

The liquid fed direct methanol fuel cell (DMFC) is considered a potential power source for both stationary and transportation applications because of its simple construction, easy operation, use of liquid fuel and its high efficiency [1,2]. However, obstacles still prevent its widespread commercial application [3–5], these include: low activity of the methanol electro-oxidation catalysts, methanol crossover from the anode to the cathode and carbon dioxide gas generation and management.

Unlike other fuel cells, the liquid fed DMFC suffers from mass transport limitations predominantly at the anode due to the low diffusion coefficient of methanol in water and the release of carbon dioxide gas bubbles [5]. A methanol concentration gradient exists within the thickness of the catalyst layer, which results a poor utilization of the catalyst [6]. In addition, a methanol diffusion limiting current is found in DMFCs using a low concentration methanol solution [7], which prevents a high power density. Therefore, the conventional anode structure based on the gas diffusion electrode employed in a proton exchange membrane fuel cell is not good for transport of methanol and carbon dioxide. Lately, a novel anode structure prepared by thermal decomposition of the corresponding metal chloride solutions onto a titanium substrate has been developed [8–10]. In this structure, a fine Ti mesh, which benefit the methanol transfer and carbon dioxide removal, is used as a substitute for the conventional gas diffusion layer in the anode. This paper further deals with the characterization of anodes with varying Pt:Ru atomic ratios for methanol oxidation.

It is well known that the ratio of Pt to Ru has a dramatic effect on the performance of the catalyst for methanol oxidation. Iwasita et al. [11] showed that the activity of smooth Pt–Ru electrodes with Ru contents between 10 and 40 at.% were similar. Gasteiger et al. [12] proposed an optimum surface composition near 10 at.% Ru at room temperature based on the need for having three sites on Pt for methanol adsorption. Chu and Gilman [13] reported a maximum in activity for 50 at.% Ru between 25 and 65 °C. Some results indicated that the optimum surface composition was ca. 20 at.% Ru [14], 40 at.% Ru [15], and 50 at.% [16,17] for unsupported Pt–Ru alloy.

Although much work has been performed on Pt–Ru catalysts for methanol oxidation, including unsupported Pt–Ru alloys [16,18,19] and Pt–Ru supported on carbon [20–22], very few have investigated the electrodes with the catalyst layer coated onto a Ti mesh by thermal decomposition for methanol oxidation. In this work, $PtRuO_2$/Ti anodes with varying Pt:Ru ratios

* Corresponding author. Tel. +86 411 84379669; fax: +86 411 84665057.
** Corresponding author.
E-mail addresses: zhgshao@dicp.ac.cn (Z.-G. Shao), wenfeng.lin@ncl.ac.uk (W.-F. Lin).
[1] Present address: Transformer Examining and Repairing Department of Nantong Power Supply Company, No. 90, South Yuelong Road, Nantong, Jiangsu 226006, PR China. Tel.: +86 513 5163619.

0378-7753/$ – see front matter © 2006 Elsevier B.V. All rights reserved.
doi:10.1016/j.jpowsour.2006.06.037

were prepared by thermal deposition of the $PtRuO_2$ catalyst layer onto a Ti mesh. The morphology and structure of the catalyst layers are analyzed by SEM, EDX, and XRD. The relative activities of the $PtRuO_2$/Ti electrodes are assessed and compared by half-cell tests and single DMFC experiments.

2. Experimental

2.1. Anode preparation

The hydrophilic anodes were prepared by direct deposition of the $PtRuO_2$ catalyst onto titanium mesh with a thermal decomposition method. The procedure was as follows: first, Ti mesh was immersed in 10% oxalic acid at 80 °C for 1 h, then rinsed with Millipore water (18 MΩ cm). The mesh was then dipped into the catalyst precusor solution and allowed to dry in air. This process was repeated several times until the desired catalyst loading was achieved. The precursor solution was a mixture of H_2PtCl_6 and $RuCl_3$ (0.2 M) in isopropanol. Afterwards, calcination was performed in air at 450 °C in a ceramic tube furnace for 1 h. Finally, the electrode was allowed to cool down to room temperature and weighed. The electrodes so prepared are denoted as $PtRuO_2$/Ti. The loading of $PtRuO_2$ catalyst in the electrode was about 2 mg cm^{-2} for the half-cell tests. For single DMFC testing, the loading of PtRu catalyst in the electrode was calculated as 4 mg cm^{-2}.

2.2. Half-cell tests

Half-cell performance testing was performed in a conventional three-electrode cell. The reference electrode was a silver/silver chloride (Ag/AgCl) electrode in saturated KCl, which was connected to the cell by a glass capillary. In this paper, unless otherwise specified, all electrode potentials are quoted versus the Ag/AgCl reference electrode. Its potential versus RHE is 0.199 V at room temperature. The counter electrode was a 2.5 cm × 2.5 cm Pt foil. The working electrode was a 1 cm × 0.5 cm Ti mesh coated with $PtRuO_2$ catalyst. A Voltlab PGZ301 Dynamic-EIS was used to control potential/current.

First, cyclic voltammetry was carried out on all of the anodes in N_2-flushed 0.5 M H_2SO_4 with and without added 0.5 M CH_3OH at room temperature (20 °C) and 60 °C. The electrodes were cycled between −0.2 and 0.7 V at a scan rate of 50 mV s^{-1} until the stable state of the electrode was reached. And then linear sweep voltammetry (LSV) was performed for the anodes in N_2-deaired 0.5 M H_2SO_4 in the presence of 0.5 M CH_3OH between −0.2 and 0.5 V at a scan rate of 1 mV s^{-1}.

2.3. Preparation of membrane electrode assembly (MEA)

The cathodes were prepared according to the procedure used in reference [23]. A Teflonised (20%) Toray TGPH-090 carbon paper with a thin microporous layer of uncatalysed (XC-72R) carbon, bound with 50 wt.% PTFE was used as the diffusion layer, and a mixture including catalysts (50% Pt/C, Johnson Matthey), 30 wt.% Nafion in *iso*-propanol was spread on the diffusion layer as the catalyst layer. The $PtRuO_2$/Ti electrodes were used as the anodes after being sprayed on 5 wt.% Nafion solution (EW 1100), equivalent to a dry Nafion loading of about 0.6 mg cm^{-2}. The cathodes and anodes were placed either side of a pre-treated Nafion 117 membrane (Aldrich). This pretreatment involved heating the membrane at 80 °C for 2 h in 3 vol.% H_2O_2 and 2 h in 0.5 M H_2SO_4 before washing in boiling Millipore water for 2 h. The assembly was hot-pressed at 70 kg cm^{-2} for 3 min at 135 °C.

2.4. Single cell tests

For single cell testing, the geometrical area of all the anodes and cathodes was ca. 6.25 cm^2 and the catalyst loading of all the anodes and cathodes were 4 and 3.5 mg cm^{-2}, respectively. Details of the testing system of the single fuel cell were described fully elsewhere [24]. A dilute methanol solution was fed to the anode inlet at a flow rate of 10 ml min^{-1} by a peristaltic pump without pre-heating and back-pressure. Room temperature and atmospheric oxygen gas was fed to the cathode inlet at a flow rate of 200 ml min^{-1} without pre-heating and humidification.

2.5. Physico-chemical characterization

A Jeol JSM-5300LV scanning electron microscope (SEM) was employed to investigate the structures and morphology of the mesh electrodes. Energy dispersive X-ray (EDX) spectroscopy was also employed for the characterisation of the electrodes by a RONTEC spectrometer (made in Germany).

X-ray diffraction (XRD) patterns were obtained on a Philips Xpert Pro diffractometer operating at 40 kV accelerating voltage and 40 mA of beam current, and using Cu $K\alpha_1$ radiation. Diffraction peaks were attributed following the Joint Committee of Powder Diffraction Standards (JCPDS) cards.

3. Results and discussion

3.1. Electrode preparation and characterization

The relative content of surface Ru sites in the $PtRuO_2$/Ti as a function of Ru/(Pt + Ru) atomic ratio in precursor solution

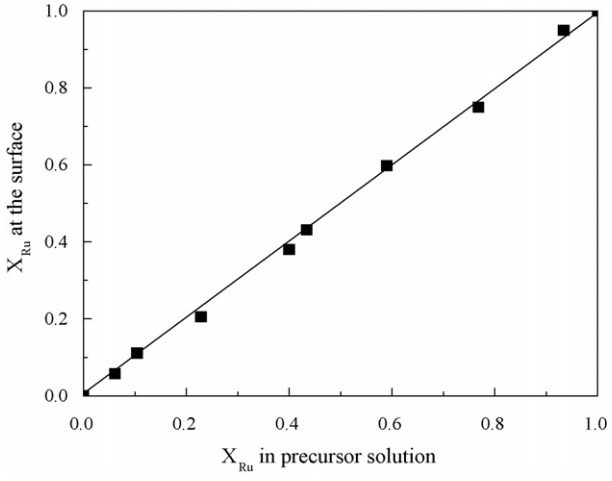

Fig. 1. Surface concentration of Ru on $PtRuO_2$/Ti vs. the concentration in the precursor solution.

is reported in Fig. 1. The Ru content of $PtRuO_2$/Ti surface is measured by EDX. From Fig. 1, a straight line with the slope angle of 45° is observed. It means that, in our experiment, the Ru content of $PtRuO_2$/Ti surface is nearly the same as that in precursor solution. This implies that the thermal decomposition method is convenient to control the catalyst loading and composition of Pt:Ru atomic ratio. Arico et al. [15] reported that a Pt surface enrichment was observed for the Pt–Ru alloy with low

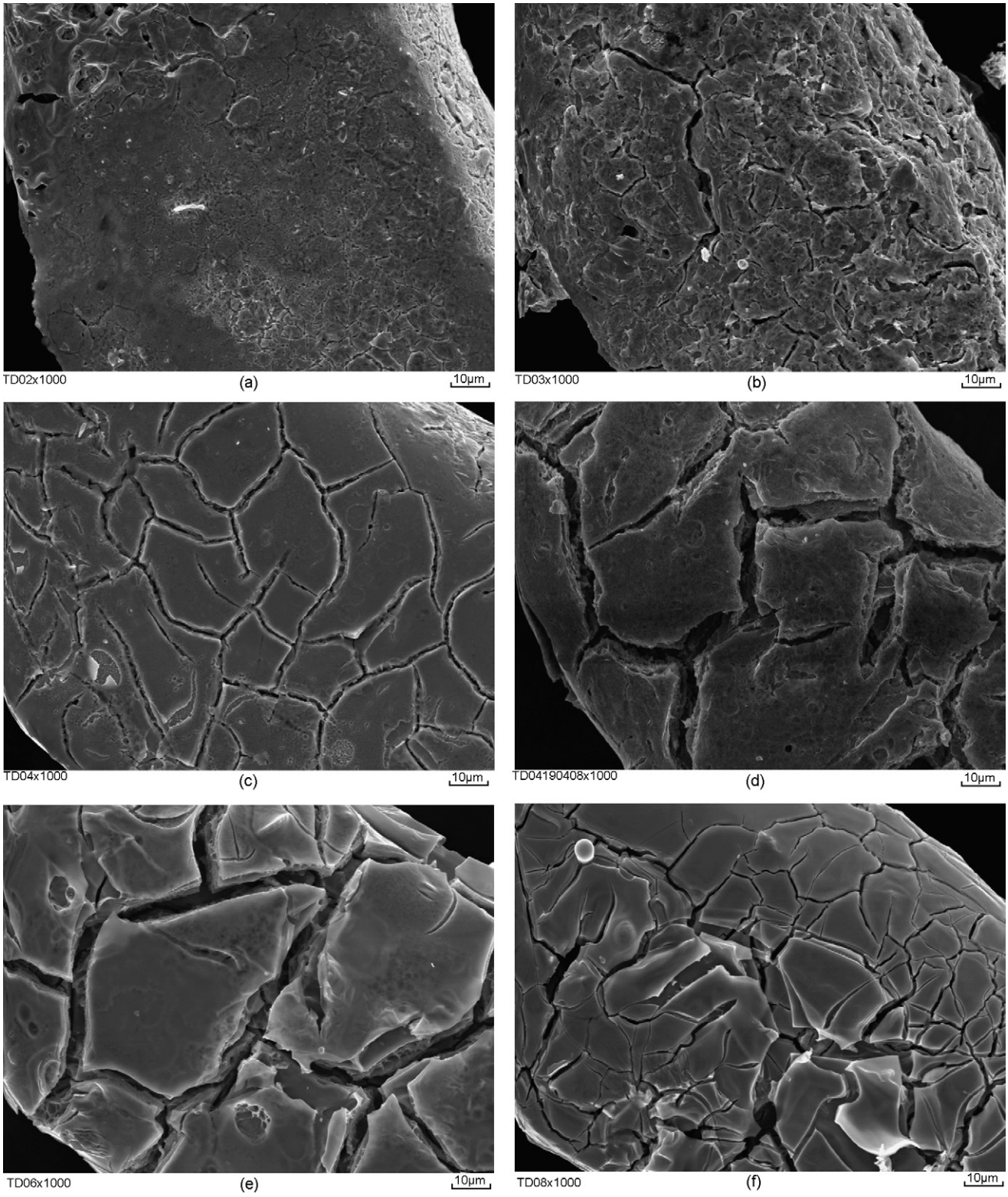

Fig. 2. SEM micrographs of the $PtRuO_2$/Ti anodes with: (a) 5.7 at.% Ru; (b) 11 at.% Ru; (c) 20 at.% Ru; (d) 38 at.% Ru; (e) 60 at.% Ru; (f) 95 at.% Ru on the catalyst layer surface.

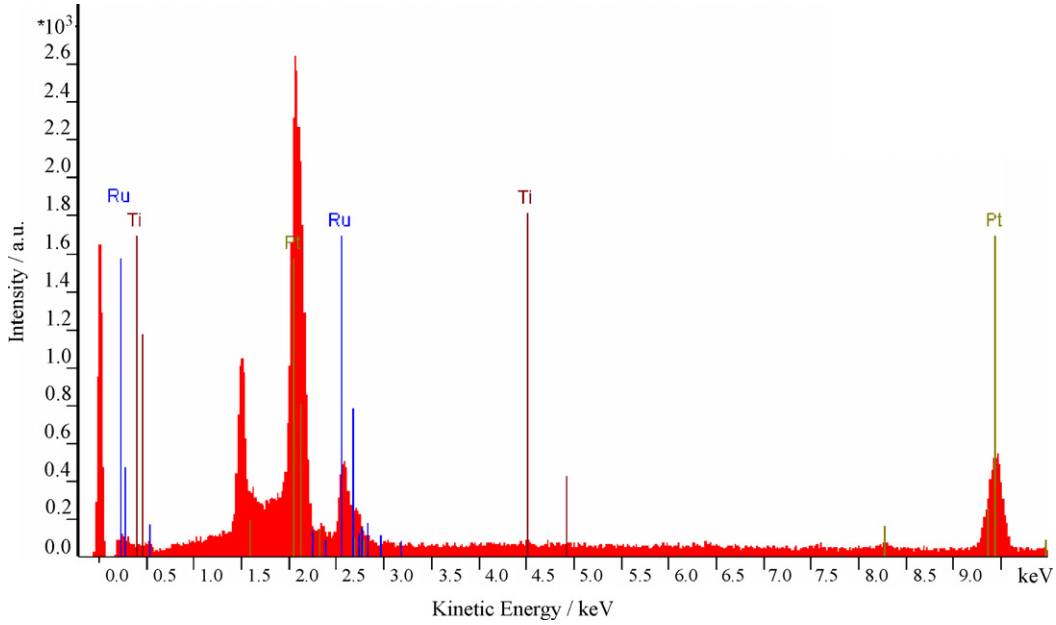

Fig. 3. EDX spectral analysis of the $PtRuO_2$/Ti.

Ru content in the bulk. It is different from our results. This can be explained by the fact that the conditions of catalyst preparation are different. In our experiment, the $PtRuO_2$/Ti electrodes were prepared at high temperature in air. This oxidative treatment will lead to a pronounced Ru surface enrichment due to the much stronger Ru–O bonds as compared with Pt–O [18]. This effect may counteract the influence of a Pt surface enrichment in Pt–Ru alloy, so the Ru content of $PtRuO_2$/Ti surface is nearly equal to that in precursor solution.

Fig. 2 shows SEM images of the $PtRuO_2$/Ti electrodes with different Pt:Ru atomic ratio. It is seen that there are many cracks in the catalyst surface, which may be formed during the decomposition of chlorine compounds and evaporation of 2-propanol. The surface of the coating layer with low Ru content is smooth, and the cracks on the surface are small. The coating becomes porous and the cracks become wide when the Ru content in the coating layer increases. This effect may be attributed to the difference of the decomposition rate between H_2PtCl_6 and $RuCl_3$.

A typical EDX spectrum is shown in Fig. 3, and the atomic ratio of Ru/(Pt + Ru) is about 38%. The characteristic peak of Ti cannot be found in Fig. 3. This indicates that the Ti mesh is almost fully covered by the $PtRuO_2$ catalyst layer. The XRD results of plain Ti mesh, commercial Pt–Ru black, and the $PtRuO_2$/Ti are shown in Fig. 4. From XRD pattern of commercial Pt–Ru black in Fig. 4, it is clearly observed that typical peaks of the bimetallic Pt–Ru alloy phase are: 40.7°, 46.6°, 69.1°, and 82.7° in 2θ, and typical peaks of the Ti substrate are also clear visible. For the $PtRuO_2$/Ti electrodes, the peaks of the Pt–Ru alloy phase are at 40.0°, 46.3°, 67.7°, and 82.0° in 2θ, and they are at lower 2θ angles than that of the commercial Pt–Ru black. This implies that the former has a larger lattice parameter and less Ru content than the latter according to Vegard's law [25]. It is also noticeable that the peaks at 28.0°, 35.0°, and 54.3° in 2θ are found from XRD pattern of the $PtRuO_2$/Ti, which indicates that PtO_2 and/or RuO_2 are formed in the $PtRuO_2$/Ti electrodes, as the peak positions of β-PtO_2 and RuO_2 are almost the same. Jang and Rajeshwar [26] studied the thermal analysis of $RuCl_3 \cdot nH_2O$ and H_2PtCl_6, and found that the decomposition temperature of $RuCl_3 \cdot nH_2O$ was about 350–450 °C, and the major thermolysis product in air was RuO_2; whilst the decomposition temperature of H_2PtCl_6 was at about 400–600 °C, and the major thermolysis product in air was Pt. In our experiments, the $PtRuO_2$/Ti electrodes were prepared at 450 °C. Therefore, the oxide species in the catalyst on the $PtRuO_2$/Ti electrodes were RuO_2. The mean particle size of the agglomerates were evaluated from the line broadening of the (2 2 0) peaks by using the Scherrer formula. These were estimated to be about 2.6 and 4.1 nm for the commercial Pt–Ru black and the thermally decomposed catalyst, respectively. The particle size of the thermally decomposed catalyst is slightly bigger than that of the commercial Pt–Ru black. It may be explained by the fact that the former is prepared at a

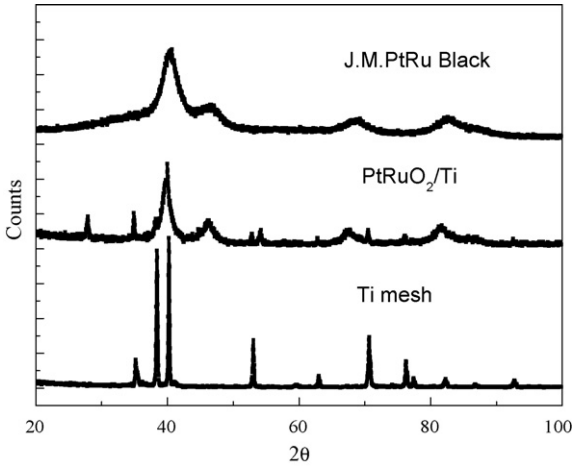

Fig. 4. XRD pattern of Ti mesh, the $PtRuO_2$/Ti electrode, and unsupported Pt–Ru black (atomic ratio Pt:Ru = 1:1) from Johnson Matthey.

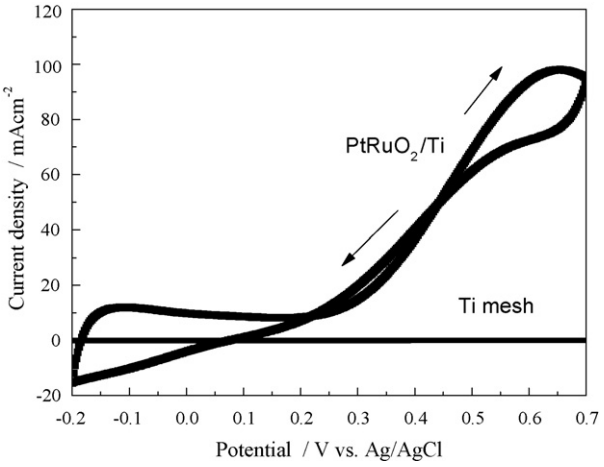

Fig. 5. Steady-state cyclic voltammograms of Ti mesh and $PtRuO_2$/Ti (44 at.% Ru) in 0.5 M H_2SO_4 + 0.5 M CH_3OH; scan rate 50 mV s^{-1}, room temperature.

higher temperature (450 °C) than the latter. The concentration of the precusor solution has a significantly effect on the particle size and activity of the catalyst. This will be published in another paper [27]. In order to reduce the influence of the concentration of the precursor solution, in our experiments, the concentration of precursor solution was fixed at 0.2 M which included both H_2PtCl_6 and $RuCl_3$.

3.2. Half-cell tests

Fig. 5 compares the CVs of the $PtRuO_2$/Ti and Ti mesh in the presence of 0.5 M H_2SO_4 + 0.5 M CH_3OH, and it is clearly seen that titanium has little activity of methanol oxidation and the effect of the plain Ti mesh can be neglected. The onset potential of methanol oxidation is observed at around 200 mV for $PtRuO_2$/Ti anode. Linear sweep voltammetries for the $PtRuO_2$/Ti electrode with 38 at.% Ru in 0.5 M H_2SO_4 + 0.5 M CH_3OH at 20 and 60 °C are shown in Fig. 6. From Fig. 6, it is seen that the activity of the methanol oxidation for $PtRuO_2$/Ti electrode markedly increases with the operating temperature. This result is to be expected from the increase of methanol oxidation kinetics with temperature.

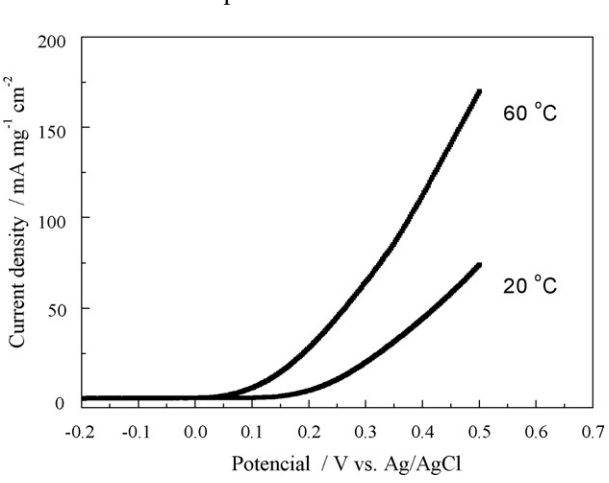

Fig. 6. Linear sweep voltammetries for the $PtRuO_2$/Ti with 38 at.% Ru in 0.5 M H_2SO_4 + 0.5 M CH_3OH; scan rate 1 mV s^{-1}.

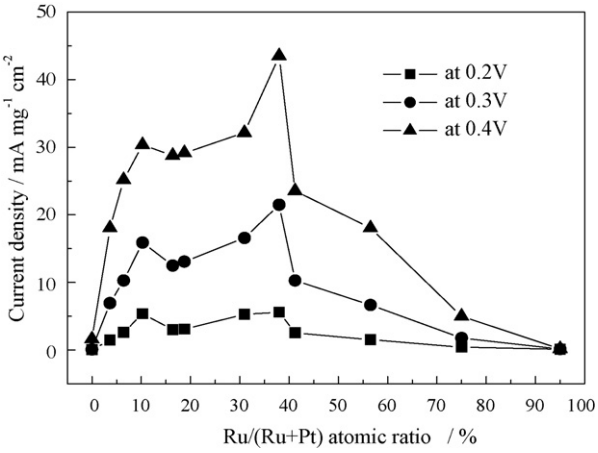

Fig. 7. Activity of the $PtRuO_2$/Ti as a function of Ru/(Pt + Ru) atomic ratio, taken from LSVs (scan rate = 1 mV s^{-1}, $PtRuO_2$ loading around 2 mg cm^{-2}, 0.5 M H_2SO_4 + 0.5 M CH_3OH) at 20 °C. The activities were calculated on the basis of the $PtRuO_2$ total loading.

Fig. 7 shows mass activities of methanol oxidation for the $PtRuO_2$/Ti electrodes at constant potentials of 0.2, 0.3, and 0.4 V versus Ag/AgCl during linear sweep voltammetry measurements as a function of Ru/(Ru + Pt) atomic ratio at 20 °C. The atomic ratio of Ru and Ru + Pt is obtained by EDX measurements. The potentials 0.2, 0.3 and 0.4 V are chosen because these covered the practical DMFC operating range. As may be seen from Fig. 7, two peaks are found in the plots, one is at 10 at.%, anther one is at 38 at.%. Moreover, the optimum Ru/(Pt + Ru) atomic ratio at room temperature is 38 at.% with separately highest output current densities of 5.6, 21.6 and 44.9 mA mg^{-1} cm^{-2} at 0.2, 0.3 and 0.4 V, respectively. This feature is consistent with that reported by Arico et al. [15], they found the optimum surface composition was ca. 40 at.% Ru for unsupported PtRu alloy as anode catalyst in DMFC. However, the activity of $PtRuO_2$/Ti electrodes with Ru contents between 10 and 38 at.% is better than that with Ru <10 at.% and Ru >38 at.%. This is in agreement with the results reported by Iwasita et al. [11]. Nevertheless, Gasteiger et al. [12] reported an optimum surface composition was near 10 at.%. Chu and Gilman [13] reported a maximum in activity for 50 at.% Ru in the bulk between 25 and 65 °C. This can be explained by the fact that the conditions of catalyst preparation and the electrolyte are different.

The mass activities for the $PtRuO_2$/Ti electrodes at 60 °C observed at constant potentials of 0.2, 0.3, and 0.4 V have been plotted versus the Ru at.% content in the catalysts surface (Fig. 8). As shown in Fig. 8, it is observed that the change in methanol oxidation behavior is remarkable, and the electrode with 38 at.% Ru content displays a best performance. It is also interesting to note that the optimum range of Ru content with good activity shifts from 10–38 at.% at 25 °C to 38–56 at.% at 60 °C. This may be interpreted on the basis of the well known, bifunctional mechanism of methanol oxidation [13,17,28–30]. According to this mechanism, Pt is the species responsible for dissociative dehydrogenation of methanol, while the Ru sites provide a source of oxygenated species for removal of carbon containing fragments. The chemisorption and subsequent dehy-

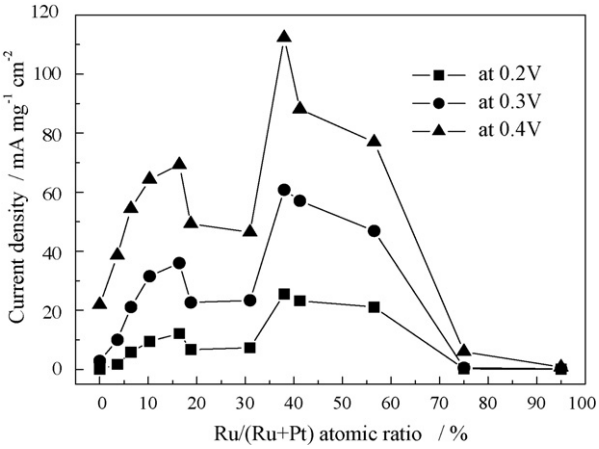

Fig. 8. Activity of the $PtRuO_2$/Ti as a function of Ru/(Pt + Ru) atomic ratio, taken from LSVs (scan rate = 1 mV s^{-1}, $PtRuO_2$ loading around 2 mg cm^{-2}, 0.5 M H_2SO_4 + 0.5 M CH_3OH) at 60 °C. The activities were calculated on the basis of the $PtRuO_2$ total loading.

drogenation of methanol on Ru sites is significantly less favored than on Pt sites, but is strongly activated by temperature [31,32]. So a Ru rich sample might be expected to perform better at higher operating temperature.

3.3. Single cell performance

Fig. 9 shows the comparison of the performance of DMFCs at 20 °C with the different anodes using aqueous 0.5 M methanol as the anode feed and atmospheric oxygen gas as the cathode feed. As shown in Fig. 9, the best performance was obtained by using the anode with a 38 at.% Ru content, followed by 10 and 50 at.% Ru. This activity sequence is consistent with that obtained in above half-cell tests.

The effect on the performance of DMFCs of raising the temperature to 60 °C is demonstrated in Fig. 10. It is seen that the cell with 38 at.% Ru anode still displays the best performance. However, the cell with 50 at.% Ru anode displays a superior performance to that with 10 at.% Ru anode. It indicates that there

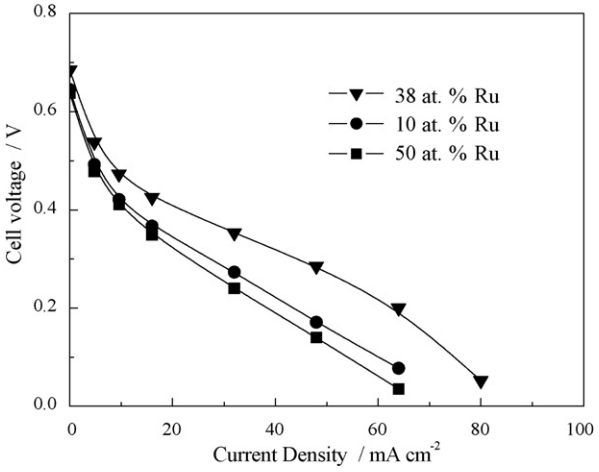

Fig. 9. Polarization curves for DMFCs with different $PtRuO_2$/Ti anodes at 20 °C, with atmospheric oxygen gas feed at the cathode (200 ml min^{-1}) and 0.5 M CH_3OH feed at the anode.

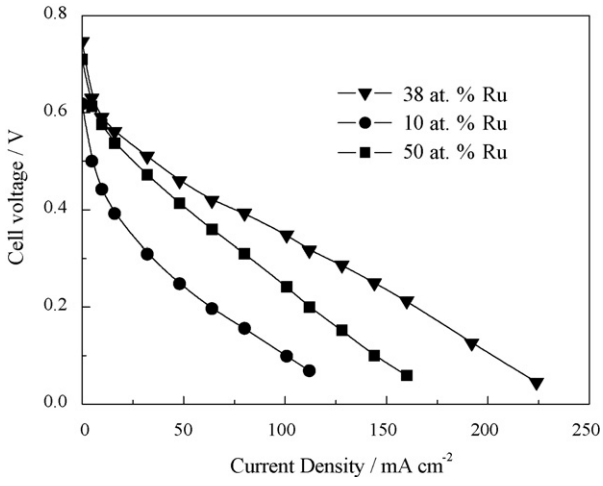

Fig. 10. Polarization curves for DMFCs with different $PtRuO_2$/Ti anodes at 60 °C, with atmospheric oxygen gas feed at the cathode (200 ml min^{-1}) and 0.5 M CH_3OH feed at the anode.

are significant temperature effects on the activity of the 50 at.% Ru anode.

4. Conclusions

$PtRuO_2$/Ti anodes with varying Pt:Ru ratios have been prepared by thermal deposition of the catalyst directly onto Ti mesh for a liquid fed DMFC. The thermal decomposition method was found to be convenient to control the catalyst loading and the Pt:Ru atomic ratio. The catalysts showed oxide and alloy characteristics as determined by XRD. It was found that the surface composition of $PtRuO_2$/Ti anodes had a significant influence on the performance of the DMFCs. The optimum Ru surface coverage is ca. 38% for a DMFC operating in the range 20–60 °C.

Acknowledgments

The authors would like to acknowledge the funding from EU (Framework 5 craft-1999-71238) and the Knowledge Innovation Program of the Chinese Academy of Sciences (Grant no. DICPR200502).

References

[1] X. Ren, M.S. Wilson, S. Gottesfeld, J. Electrochem. Soc. 143 (1996) L12.
[2] D. Kim, E.A. Cho, S.-A. Hong, I.-H. Oh, H.Y. Ha, J. Power Sources 130 (2004) 172.
[3] A.S. Arico, V. Baglio, E. Modica, A. Di Blasi, V. Antonucci, Electrochem. Commun. 6 (2004) 164.
[4] Z.-G. Shao, X. Wang, I.-M. Hsing, J. Membr. Sci. 210 (2002) 147.
[5] H. Yang, T.S. Zhao, Q. Ye, J. Power Sources 139 (2005) 79.
[6] M. Wohr, S.R. Narayanan, G. Halpert, Abstract 797, The Electrochemical Society Meeting Abstracts, vol. 96-2, San Antonio, TX, October 6–11, 1996.
[7] K. Scott, W.M. Taama, S. Kramer, P. Argyropoulos, K. Sundmacher, Electrochim. Acta 45 (1999) 945.
[8] P.G. Allen, S.D. Conradson, M.S. Wilson, S. Gottesfeld, I.D. Raistrick, J. Valerio, M. Lovato, Electrochim. Acta 39 (1994) 2415.
[9] Z.-G. Shao, W.-F. Lin, F. Zhu, P.A. Christensen, M. Li, H. Zhang, Electrochem. Commun. 8 (2006) 5.

[10] C. Lim, K. Scott, R.G. Allen, S. Roy, J. Appl. Electrochem. 34 (2004) 929.
[11] T. Iwasita, H. Hoster, A. John-Anacker, W.F. Lin, W. Vielstich, Langmuir 16 (2000) 522.
[12] H.A. Gasteiger, N. Markovic, P.N. Ross Jr., E.J. Cairns, J. Electrochem. Soc. 141 (1994) 1795.
[13] D. Chu, S. Gilman, J. Electrochem. Soc. 143 (1996) 1685.
[14] B.A.L. de Mishima, H.T. Mishima, G. Castro, Electrochim. Acta 40 (1995) 2491.
[15] A.S. Arico, P.L. Antonucci, E. Modica, V. Baglio, H. Kim, V. Antonucci, Electrochim. Acta 47 (2002) 3723.
[16] M.-S. Loffler, H. Natter, R. Hempelmann, K. Wippermann, Electrochim. Acta 48 (2003) 3047.
[17] M. Watanabe, S. Motoo, J. Electroanal. Chem. 60 (1975) 275.
[18] Z. Jusys, J. Kaiser, R.J. Behm, Electrochim. Acta 47 (2002) 3693.
[19] J. Solla-Gullon, F.J. Vidal-Iglesias, V. Montiel, A. Aldaz, Electrochim. Acta 49 (2004) 5079.
[20] J.W. Guo, T.S. Zhao, J. Prabhuram, R. Chen, C.W. Wong, Electrochim. Acta 51 (2005) 754.
[21] L. Jiang, G. Sun, X. Zhao, Z. Zhou, S. Yan, S. Tang, G. Wang, B. Zhou, Q. Xin, Electrochim. Acta 50 (2005) 2371.
[22] Y. Takasu, T. Kawaguchi, W. Sugimoto, Y. Murakami, Electrochim. Acta 48 (2003) 3861.
[23] C. Lim, C.Y. Wang, J. Power Sources 113 (2003) 145.
[24] R.W. Reeve, P.A. Christensen, A.J. Dickinson, A. Hamnett, K. Scott, Electrochim. Acta 45 (2000) 4237.
[25] E. Antolini, Mater. Chem. Phys. 78 (2003) 563.
[26] G.-W. Jang, K. Rajeshwar, J. Electrochem. Soc. 134 (1987) 1830.
[27] Z.-G. Shao, F. Zhu, W.-F. Lin, P.A. Christensen, H. Zhang, B. Yi, J. Electrochem. Soc. 153 (2006) A1575.
[28] V.S. Bagotzky, Y.B. Vassilyev, Electrochim. Acta 12 (1967) 1323.
[29] K.A. Friedrich, K.-P. Geyzers, U. Linke, U. Stimming, J. Stumper, J. Electroanal. Chem. 402 (1996) 123.
[30] T. Frelink, W. Visscher, J.A.R.V. Veen, Langmuir 12 (1996) 3702.
[31] S. Wasmus, A. Kuver, J. Electroanal. Chem. 461 (1999) 14.
[32] K.A. Friedrich, K.P. Geyzers, A.J. Dickinson, U. Stimming, J. Electroanal. Chem. 524-525 (2002) 261.